Synthesis and Magnetic Characterizations of Manganite-Based Composite Nanoparticles for Biomedical Applications

R. Bah, K.Zhang, T. Holloway, R. B. Konda, R. Mundle, H. Mustafa,
R. R. Rakhimov, and A. K. Pradhan
Center for Materials Research, Norfolk State University, 700 Park Avenue,
Norfolk, Virginia 23504, USA

Xiaohui Wei and D. J. Sellmyer
Department of Physics and Astronomy and Center for Materials Research and Analysis,
University of Nebraska, Lincoln, Nebraska 68588-0113, USA

ABSTRACT

Chemically synthesized highly crystalline lanthanum strontium manganite $LaSrMnO_3$ and Eu-doped Y_2O_3 and their composites yielding nanoparticles of size 30–40 nm are reported in this paper. Magnetic measurements performed on the synthesized nanoparticles and composites showed a magnetic transition at about 370 K with a superparamagnetic behavior at room temperature. The ferromagnetic resonance studies of the nanoparticles showed large linewidth due to surface strains. The composite nanoparticles also displayed luminescent behavior when irradiated with ultraviolet light. The manganites as well as their composite with the luminescent nanoparticles may be very useful for biomedical applications. For this possible application, the nature and effects of the nanoparticles in a biological environment have been studied as such particles are known to be toxic.

Keywords: *Magnetic nanoparticles, Toxicity studies, Biomedical applications*

I. INTRODUCTION

Magnetic nanoparticles with a Curie temperature above room temperature are needed for most biomedical and magnetofluidic applications. Rare-earth based group of half-metallic ferromagnetic materials, such as manganites with a typical composition $La_{0.7}Sr_{0.3}MnO_3$ (LSMO), are of interest in this context due to its high T_C of 380 K and a large magnetic moment at room temperature.[1–5] The half-metallic manganites are fairly metallic and can have large microwave absorption with the possibility of its use in hyperthermia applications and the large moment can also allow its use in marker experiments in biodetection[6] as well. On the other hand, due to significant magnetoresistance effects in the immediate vicinity of the Curie point of manganites, eddy currents can be utilized as part of the heating mechanism. Hence, one can achieve the selective warming of the given areas of an organism by T_c-limiting production of controlled heat effects by means of an alternating external magnetic field. In general, particles that switch certain inherent properties "on/off" in relation to the relatively simple parameter, such as temperature, will provide possibilities for many potential designs of biomedical applications.

Another interesting material is Eu^{3+} ions, which show luminescent properties due to $^5D_0 \rightarrow {}^7F_2$ transitions within and emits red light with a wavelength of 611 nm, and can be used as the red phosphor. Y_2O_3:Eu^{3+} has a lumen equivalent brightness of 70% relative to 611 nm light and radiant efficiency of about 8.7% with better saturation without any detrimental effects.[7,8] With the rapid advancement of biotechnology, nanoparticles of doped lanthanide oxides can be used as promising labels because of their above mentioned optical properties, lack of photobleaching, and long luminescence lifetime (~1 ms).

Coating the nanoparticles with a suitable material offers the possibility of attaching them to antibodies, proteins, medical drugs, etc. Therefore, studies on surface adsorption, the possibility of functionalizing and/or conjugating the particle coating with bioactive components, is also a crucial issue. There are only a few reports available for the synthesis of stochiometric manganite nanoparticles.[9,10] Here, we report the synthesis and characterization of

NSTI-Nanotech 2008, www.nsti.org, ISBN 978-1-4200-8503-7 Vol. 1

macromolecule encapsulated LSMO and Eu:Y_2O_3 composite nanoparticles.

2. EXPERIMENTS

$La_{0.7}Sr_{0.3}MnO_3$ (hence called as LSMO) nanoparticles were synthesized by a sol-gel method from their acetate hydrate precursors, which were dissolved in water. This solution was mixed with citric acid solution in 1:1 volume ratio ultrasonically for about 30 min. The mixture was heated in a water bath at 80 °C until all water is evaporated, yielding a yellowish transparent gel. The gel was further heated in an oven at 100 °C which formed a foamy precursor. This precursor decomposed to give black-colored flakes of extremely fine particle size on further heating at 400 °C for 4 h. The flakes were ground and sintered at 800 °C for duration of 2 h. Further heating in O_2 ambient removed the carbon content. The nanopowders were coated with equal quantity ofoctadecyl amine (ODA) by magnetically stirring at 120 °C.

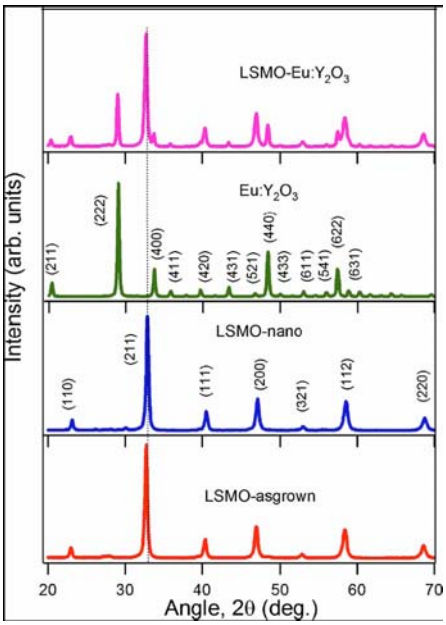

FIG. 1. X-ray diffraction patterns of LSMO, EYO, and composite nanopowders.

A solution of ODA-coated LSMO and chloroform was prepared with a molarity of 10^{-2} *M* and sonicated for 1 h for dispersion. The solution was rested for 24 h settling of the heavier LSMO particles. The solution containing suspended LSMO-ODA nanoparticles was decanted and purified using methanol several times in order to remove excess ODA from the surface. The final purification was done using magnetic separation in order to remove any carbon content in the solution.
The purified powder was naturally dried.

The nanocrystalline Eu^{3+}:Y_2O_3 (EYO) powders were synthesized using a combustion technique[11,12] from their respective nitrate solutions. LSMO and EYO nanopowders were thoroughly mixed and heated at 800 °C for 30 min to form a composite. These powders were coated with ODA and purified as described above.

3. RESULTS AND DISCUSSION

Figure 1 shows the powder x-ray diffraction (XRD) patterns of nanoparticle ensembles of manganites, doped rareearth oxides, and their composites. The purified manganite nanoparticles are highly crystalline and share the pseudocubic perovskite structure. However, the broadening of the XRD peaks is influenced by surface strain. Similar effects due to surface strains were observed in EYO nanoparticles. The XRD patterns of composite nanoparticles exhibit the characteristics of both LSMO and EYO nanoparticles.

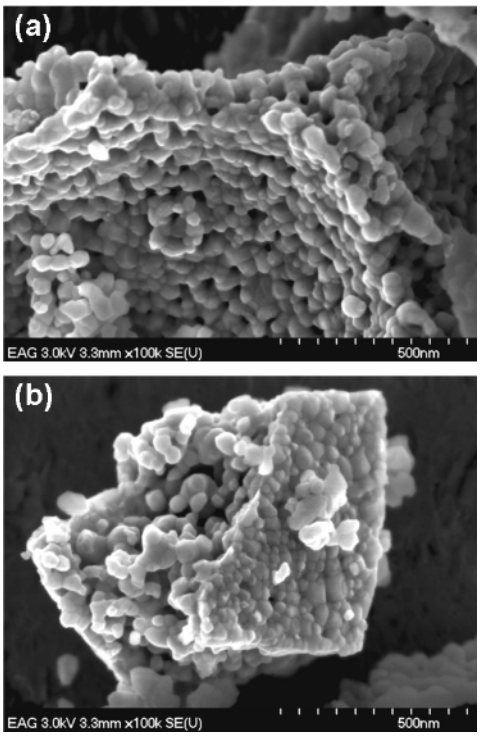

FIG. (2.a) FE-SEM image of LSMO naoparticles with and without ODA coating.

Figures (2a) and (2b) show the representative field emission scanning electron microscope (FE-SEM) images of LSMO nanoparticles with and without ODA coating. The size distribution is rather narrow, and the crystallite size is in the range of 30–40 nm. Analysis of electron diffraction from nanoparticles and XRD patterns, such as those shown in Fig. 1, indicates that both manganite and EYO nanoparticles are highly crystalline and share the pseudocubic perovskite and cubic structures, respectively.

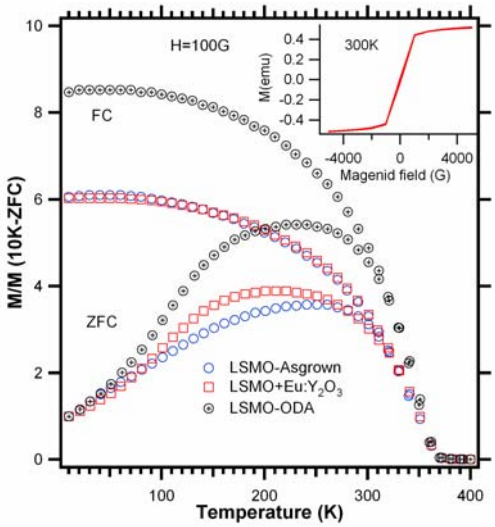

FIG. 3. Temperature dependent field-cooled (FC) and ZFC magnetization of as-synthesized LSMO, ODA-coated LSMO and composite (LSMO+EYO) nanopowders. The inset shows the magnetic hysteresis of LSMO nanoparticles.

Figure 3 shows the temperature (*T*) dependent magnetization (*M*) of LSMO and composite nanoparticles in an applied magnetic field (*H*) of 100 G. All samples show the onset of the magnetic transition at 370 K with a Curie temperature ~360 K. The as grown LSMO and LSMO+EYO composites show very similar magnetization behavior. The samples were cooled from 400 K down to 10 K under a magnetic field and then *M* was recorded as the sample was warmed to 400 K under the same magnetic field [field cooled (FC)]. Similarly, the samples were cooled from 400 K down to 10 K with zero magnetic field and then *M* was recorded as the sample was warmed to 400 K under the same magnetic field applied at 10K [zero-field cooled (ZFC)]. The results clearly illustrate the occurrence of ferromagnetic-to-paramagnetic phase transitions in all three samples as the temperature is increased. On the other hand, the coated nanoparticles showed reduced magnetization compared to LSMO due to reduction in the volume fraction caused by ODA coating, as expected in both FC and ZFC curves. The magnitude of the low temperature saturation magnetization also decreases with ODA coating, although hardly any reduction in the transition temperature was observed. Interestingly, the absolute magnetization increases in composite nanoparticles compared to that of LSMO. One of the reasons for such increase may be due to the local field enhancement at Eu site. However, further studies are necessary to resolve this issue. The slight reduction in transition temperature in these nanoparticles compared to their bulk counterpart (~375 K) may be attributed to the surface-to-volume ratio in the nanoparticles, spin disorders at the surface,[13] as well as due to the presence of superparamagnetic behavior of the nanoparticles. For nanoparticles of the order of tens of nanometers or less, one can see superparamagnetism, where the magnetic moment of the particle as a whole is free to fluctuate in response to thermal energy, while the individual atomic moments maintain their ordered state relative to each other, yielding anhysteretic, but sigmoidal *M*-*H* curve. In fact, the superparamagnetic behavior is observed in these nanoparticles, and a magnetic field dependent magnetization curve is presented in the inset of Fig. 3 for LSMO nanoparticles.

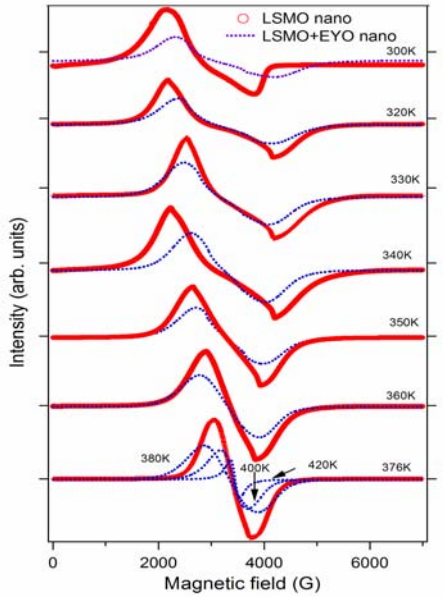

NSTI-Nanotech 2008, www.nsti.org, ISBN 978-1-4200-8503-7 Vol. 1

FIG. 4. Ferromagnetic resonance spectra of LSMO and composite (LSMO+EYO) nanopowders.

Figure 4 shows the ferromagnetic resonance (FMR) spectra of LSMO and composite nanoparticles at various temperatures. FMR studies are probably the most sensitive method for detecting ferromagnetic order as well as the possible existence of other magnetic species. The narrower linewidth is generally taken as a signature of a homogeneous sample. However, a large FMR linewidth, which is in the range of ~2 kG, indicates the effects of surface strains due to the size effect of the nanoparticles. No significant difference in the FMR curves was noticed, except a slight increase in resonance field in EYO nanoparticles. However, a striking difference is the shape of the FMR resonance curve, which loses the ferromagnetic feature as the temperature is increased beyond 350K. This can be attributed due the interface effects in the composite nanoparticles.

4. CONCLUSION

We synthesized LSMO and macromolecule encapsulated LSMO and Eu:Y_2O_3 composite nanoparticles by the chemical routes. Both nanopowders show very good crystalline quality. The composite nanopowders of LSMO and Eu:Y_2O_3 were synthesized by mixing and controlled heat treatment. The FE-SEM and TEM images of the individual nanoparticles and composite nanopowders show that the particles are in the range of 30–40 nm. The LSMO as grown, ODA-coated, and composite nanoparticles show magnetic transition around 370 K. The composite nanoparticles show superparamagnetic behavior at 300 K. The FMR studies of the nanoparticles show large linewidth due to the surface strains. Our results are useful for possible applications in the field of biomedicals.

5. ACKNOWLEDGMENTS

This work is supported by NSF (RISE) project. Research at the University of Nebraska is supported by NSF-MRSEC, ONR, and CMRA.

6. REFERENCES

1. S. S. Davis, Trends Biotechnol. **15**, 217, 1997.
2. H. Y. Hwang, S. W. Cheong, N. P. Ong, and B. Batlogg, Phys. Rev. Lett. **77**, 2041 (1996).
3. A. Chainani, M. Mathew, and D. D. Sarma, Phys. Rev. B **47**, 15397 (1993).
4. Z. Trajanovic, C. Kwon, M. C. Robson, K. C. Kim, M. Rajaswari, S. E. Lofland, S. M. Bhagat, and D. Fork, Appl. Phys. Lett. **69**, 1007, 1996.
5. J. M. De Teresa, C. Marquina, D. Serrate, R. Fernandez-Pacheco, L. Morellon, P. A. Algarabel, and M. R. Ibarra, Int. J. Nanotechnol. **2**, 3 (2005).
6. A. Pankhurst, J. Connolly, S. K. Jones, and J. Dobson, J. Phys. D **36**, R167 (2003).
7. G. Blasse and B. C. Grabmaier, *Luminescent Materials* !Springer, Berlin, (1994).
8. T. Hase, T. Kano, E. Nakazawa, and H. Yamamoto, in *Advances in Electronics and Electron Physics*, edited by P. W. Hawkes Academic, NewYork, 1990, Vol. 79, p. 135.
9. J. J. Urban, L. Ouyang, M.-H. Jo, D. S. Wang, and H. Park, Nano Lett. **4**, 1547, 2004.
10. V. Uskokovic, A. Kocak, M. Drofenik, and M. Drofenik, Int. J. Appl. Ceram. Technol. **3**, 134, 2006; R. Rajagopal, J. Mona, S. N. Kale, T. Bala, R. Pasricha, P. Poddar, M. Sastry, B. L. V. Prasad, D. C. Kundaliya, and S. B. Ogale, Appl. Phys. Lett. **89**, 023107, 2006.
11. E. Zych, Opt. Mater. Amsterdam, Neth. **16**, 445, 2001.
12. K. Zhang, A. K. Pradhan, G. B. Loutts, U. N. Roy, Y. Cui, and A. Burger, J. Opt. Soc. Am. B **21**, 1804, 2004.
13. A. J. Millis, Nature London **392**, 147,1998.